

# Control Lyapunov Functions for Controllable Series Devices

Mehrdad Ghandhari, *Member, IEEE*, Göran Andersson, *Fellow, IEEE*, and Ian A. Hiskens, *Senior Member, IEEE*

**Abstract**—Controllable Series Devices (CSD), i.e., series-connected Flexible AC Transmission Systems (FACTS) devices, such as Unified Power Controller (UPFC), Controllable Series Capacitor (CSC) and Quadrature Boosting Transformer (QBT) with a suitable control scheme can improve transient stability and help to damp electromechanical oscillations. For these devices, a general model, which is referred to as injection model, is used. This model is valid for load flow and angle stability analysis and is helpful for understanding the impact of the CSD on power system stability. Also, based on Lyapunov theory a control strategy for damping of electromechanical power oscillations in a multi-machine power system is derived. Lyapunov theory deals with dynamical systems without inputs. For this reason, it has traditionally been applied only to closed-loop control systems, that is, systems for which the input has been eliminated through the substitution of a predetermined feedback control. However, in this paper, we use Lyapunov function candidates in feedback design itself by making the Lyapunov derivative negative when choosing the control. This control strategy is called Control Lyapunov Function (CLF) for systems with control inputs.

**Index Terms**—CSC and CLF, FACTS, QBT, UPFC.

## I. INTRODUCTION

**P**OWER systems exhibit various modes of oscillation due to interactions among system components. Many of the oscillations are due to synchronous generator rotors swinging relative to each other. In this paper, the electromechanical oscillations (initiated by faults) which typically are in the frequency range of 0.1 to 2 Hz, are considered.

In recent years, the fast progress in the field of power electronics has opened new opportunities for the power industry via utilization of the Controllable Series Devices (CSD), such as Unified Power Controller (UPFC), Controllable Series Capacitor (CSC) and Quadrature Boosting Transformer (QBT) which offer an alternative means to mitigate power system oscillations. Thus, a question of great importance is the selection of the input signals and a control strategy for these devices in order to damp power oscillations in an effective and robust manner.

Manuscript received November 2, 1999; revised February 28, 2001. This work was supported by ABB, Svenska Kraftnät, and PG & E through the Elektra Program.

M. Ghandhari is with the Royal Institute of Technology (KTH), Department of Electric Power Engineering, S-100 44 Stockholm, Sweden (e-mail: Mehrdad.Ghandhari@ekc.kth.se).

G. Andersson is with the Federal Institute of Technology (ETH), Electric Power Systems Group, ETL G26, CH-8092 Zürich, Switzerland (e-mail: andersson@eeh.ee.ethz.ch).

I. A. Hiskens is with the University of Illinois at UC, Department of Electrical and Computer Engineering, Urbana, IL 61801 USA (e-mail: hiskens@ece.uiuc.edu).

Publisher Item Identifier S 0885-8950(01)09452-4.

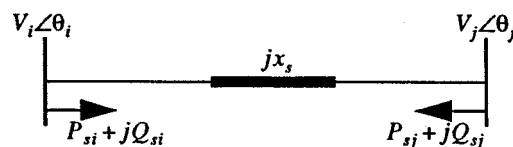


Fig. 1. The CSD injection model.

Modern power systems are large scale and complex. Disturbances typically change the network topology and result in non-linear system response. Also, because of deregulation the configuration of the interconnected grid will routinely be in a state of change. Therefore a control strategy that will counteract a wide variety of disturbances that may occur in the power system is attractive. This paper develops a control strategy for the CSD, based on the Control Lyapunov Function (CLF). The derived control strategy has the same basic structure for all CSD and it is based on input signals that easily can be obtained from locally measurable variables.

This paper is organized as follows. In Section II modeling of the CSD based on the injection model is presented. Section III describes the ideas with CLF and its application in power system. Also, a control strategy for the CSD is developed based on the CLF. We provide some numerical test results, future work and the conclusions of this paper in Sections IV–VI respectively.

## II. INJECTION MODEL

Fig. 1 shows the injection model for a CSD which is located between bus *i* and bus *j*, see [1, Chapter 4]. For UPFC and QBT,  $x_s$  is the effective reactance seen from the transmission line side of the series transformer and for CSC it is the reactance of the line in which the CSC is installed, i.e.,  $x_s = x_L$ .

In Fig. 1, for

**UPFC :**

$$P_{si} = b_s V_i V_j (u_1 \sin(\theta_{ij}) + u_2 \cos(\theta_{ij})), \quad Q_{si} = u_1 b_s V_i^2$$

$$P_{sj} = -P_{si}, \quad Q_{sj} = -b_s V_i V_j (u_1 \cos(\theta_{ij}) - u_2 \sin(\theta_{ij}))$$

**QBT :**

$$P_{si} = u_q b_s V_i V_j \cos(\theta_{ij}), \quad Q_{si} = u_q^2 b_s V_i^2 + u_q b_s V_i V_j \sin(\theta_{ij})$$

$$P_{sj} = -P_{si}, \quad Q_{sj} = u_q b_s V_i V_j \sin(\theta_{ij})$$

**CSC :**

$$P_{si} = u_c b_s V_i V_j \sin(\theta_{ij}), \quad Q_{si} = u_c b_s (V_i^2 - V_i V_j \cos(\theta_{ij}))$$

$$P_{sj} = -P_{si}, \quad Q_{sj} = u_c b_s (V_j^2 - V_i V_j \cos(\theta_{ij}))$$

where

$$\begin{aligned} b_s &= 1/x_s; \\ \theta_{ij} &= \theta_i - \theta_j; \\ u_1, u_2, u_q \text{ and } u_c &\text{ are control variables, full details are} \\ &\text{given in [1].} \end{aligned}$$

For CSC

$$u_c = \frac{x_c}{x_L - x_c}, \quad x_{c\min} \leq x_c \leq x_{c\max}. \quad (1)$$

If the CSC has a steady state set point  $x_{co}$ , then  $x_c = x_{co} + \Delta x_c$  where  $\Delta x_c$  is the control modulation. The reactance of the line in which the CSC is installed, can then be given by  $x_s = x_L^{new} = x_L - x_{co}$ . Thus,  $x_c$  in (1) is replaced by  $\Delta x_c$  with  $x_{c\min} - x_{co} \leq \Delta x_c \leq x_{c\max} - x_{co}$ .

### III. CONTROL LYAPUNOV FUNCTION

#### A. Theoretical Considerations

Power systems are most naturally described by Differential Algebraic (DA) models of the form  $\dot{x} = f(x, y)$  and  $0 = g(x, y)$ . The algebraic states  $y$  are related to the dynamic states  $x$  through the algebraic equations  $g$ . By virtue of the implicit function theorem, it can be shown that this model is locally equivalent to a differential equation model

$$\dot{x} = f(x, h(x)) = \tilde{f}(x), \quad x \in \Omega \subseteq \mathbb{R}^\eta \quad (2)$$

if  $\partial g/\partial y$  is nonsingular. Under certain modeling assumptions, e.g., constant admittance loads, local equivalence extends to global equivalence. This model has become known in the energy function literature as the Reduced Network Model (RNM). The presentation of CLF in this paper is based on (2). Most ideas extend naturally to the DA model though.

Let the origin be an equilibrium point of system (2), i.e.,  $\tilde{f}(0) = 0$ , possibly after a coordinate change. A function  $\mathcal{V}(x)$  is said to be a Lyapunov function for (2), if it is of class (at least)  $C^1$  and there exists a neighborhood  $Q$  of the origin such that

$$\mathcal{V}(x) > 0, \quad \forall x \in Q, \quad x \neq 0 \quad \text{and} \quad \mathcal{V}(0) = 0 \quad (3)$$

$$\dot{\mathcal{V}}(x) < 0, \quad \forall x \in Q, \quad x \neq 0 \quad \text{and} \quad \dot{\mathcal{V}}(0) = 0. \quad (4)$$

If (2) has a Lyapunov function then the origin is locally asymptotically stable. Conversely, for any locally asymptotically stable system, a Lyapunov function exists [2].

For mechanical and electrical systems, the physical energy (or energy-like) functions are often used as Lyapunov function candidates. The time derivatives of these energy functions are negative semidefinite. Therefore, these functions fail to satisfy condition (4) for Lyapunov function. However, applying La Salle's invariance principle or the theorems of Barbashin and Krasovskii, [2], the energy functions satisfy the asymptotic stability condition and they can be considered as Lyapunov function candidates.

Lyapunov theory deals with dynamical systems without inputs. For this reason, it has traditionally been applied only to closed-loop control systems, that is, systems for which the input has been eliminated through the substitution of a predetermined feedback control. However, some authors, [5]–[7], started using Lyapunov function candidates in feedback design itself

by making the Lyapunov derivative negative when choosing the control. Such ideas have been made precise with the introduction of the concept of a Control Lyapunov Function for systems with control input [3].

The following discussion largely follows that in [4] and references therein. Consider the control system

$$\dot{x} = f(x, u), \quad x \in \Omega \subseteq \mathbb{R}^\eta, \quad u \in \mathbb{R}^m. \quad (5)$$

We want to find conditions for the existence of a feedback control  $u = u(x)$  defined in a neighborhood of the origin such that the closed-loop system  $\dot{x} = f(x, u(x))$  has a locally asymptotically stable equilibrium point at the origin, i.e.,  $f(0, u(0)) = 0$ . If such a function  $u(x)$  exists, we say that (5) is stabilizable at the origin and the function  $u(x)$  is called a stabilizing feedback law or a stabilizer. Assume that (5) is continuously stabilizable. According to the converse Lyapunov's theorem, there must be a positive definite function  $\mathcal{V}(x)$  such that

$$\dot{\mathcal{V}}(x) = \text{grad}(\mathcal{V}) \cdot f(x, u(x)) < 0, \quad \forall x \in Q, \quad x \neq 0. \quad (6)$$

A function  $\mathcal{V}(x)$  satisfying (3) and (6) is called a Control Lyapunov Function. Next, consider the affine system

$$\dot{x} = f(x, u) = f_o(x) + \sum_{i=1}^m u_i f_i(x). \quad (7)$$

Note that  $f_o$  and  $f_i$  have the same dimension, i.e.,  $\eta \times 1$ . For sake of simplicity, we assume  $f_o(0) = 0$ , so that we can take also  $u_i(0) = 0$ . In [5], Artstein proved that there exists a stabilizer  $u_i(x)$  for (7), if and only if (7) admits a CLF. In [6], Sontag presented explicit formulas for  $u_i(x)$ . In the case of using an energy function as a Lyapunov function candidate, the treatment of system (7) fits better in the framework of the Jurdjevic–Quinn approach [7]. We say that (7) satisfies a Lyapunov condition of the Jurdjevic–Quinn type if there is a neighborhood  $Q$  of the origin and a  $C^\infty$  function  $\mathcal{V}(x)$  such that (3) holds and  $\text{grad}(\mathcal{V}) \cdot f_o(x) \leq 0$  for  $x \in Q$ . According to the Jurdjevic–Quinn approach, a stabilizing feedback law is typically defined componentwise, setting  $u(x) = [u_1(x) \cdots u_m(x)]$  and  $u_i(x) = -\text{grad}(\mathcal{V}) \cdot f_i(x)$ ,  $i = 1 \cdots m$ . Thus, the time derivative of  $\mathcal{V}(x)$  for  $x \in Q$  with respect to the closed-loop system is given by

$$\dot{\mathcal{V}}(x) = \text{grad}(\mathcal{V}) \cdot f_o(x) - \sum_{i=1}^m (\text{grad}(\mathcal{V}) \cdot f_i(x))^2 \leq 0. \quad (8)$$

To summarize, just as the existence of a Lyapunov function is necessary and sufficient for the stability of a system without inputs, the existence of a CLF is necessary and sufficient for the stabilizability of a system with a control input [3].

#### B. Application in Power System

Consider a power network which is modeled by  $2n + N$  nodes connected by lossless transmission lines which is represented by node admittance matrix  $Y = j[B_{ki}]$ . The first  $n$  nodes are the internal buses of the generators. The nodes  $n + 1$  to  $2n$  are the terminal buses of the generators where there may also be loads. Each generator terminal bus is connected with its internal bus

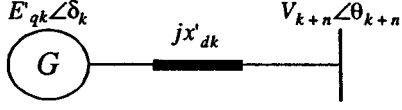


Fig. 2. Transient equivalent circuit of a generator.

through a lossless line with reactance equal to  $x'_{dk}$ , i.e., the generator transient reactance, see Fig. 2. The remaining  $N$  nodes are the load buses. It is assumed that the mechanical input power of the generator is constant. The machine model considered here is flux-decay model (one-axis model). Exciters and governors are not included in this model. The rest of the treatment follows that in [8] and references therein. The dynamics of the generators are described by the following differential equations (with respect to the COI reference frame).

For  $k = 1 \dots n$ ,

$$\begin{aligned} \dot{\delta}_k &= \tilde{\omega}_k \\ M_k \dot{\tilde{\omega}}_k &= P_{mk} - P_{ek} - D_k \tilde{\omega}_k - \frac{M_k}{M_T} P_{COI} \\ T'_{dok} \dot{E}'_{qk} &= \frac{x_{dk} - x'_{dk}}{x'_{dk}} V_{k+n} \cos(\delta_k - \theta_{k+n}) \\ &\quad + E_f dk - \frac{x_{dk}}{x'_{dk}} E'_{qk} \end{aligned} \quad (9)$$

where  $P_{COI} = \sum_{k=1}^n (P_{mk} - P_{ek})$  and  $P_{ek}$  is the generated electrical power. Full details are given in [8]. For the lossless system the following equations can be written at bus  $k$  where  $P_k$  is the real power and  $Q_k$  is the reactive power injected into the system from bus  $k$ .

For  $k = (2n + 1) \dots (2n + N)$

$$\begin{aligned} P_k &= \sum_{l=n+1}^{2n+N} B_{kl} V_k V_l \sin(\theta_k - \theta_l) \\ Q_k &= - \sum_{l=n+1}^{2n+N} B_{kl} V_k V_l \cos(\theta_k - \theta_l). \end{aligned}$$

For  $k = (n + 1) \dots 2n$ ,  $P_k$  and  $Q_k$  are similar, but also take account of generated real and reactive power [8].

Real load at each bus is represented by a constant load and reactive load by an arbitrary function of voltage at the respective bus. Thus, for  $k = (n + 1) \dots (2n + N)$

$$\begin{aligned} P_{Lk} &= P_{Lk}^o \\ Q_{Lk} &= f_{qk}(V_k). \end{aligned}$$

Therefore, for  $k = (n + 1) \dots (2n + N)$  the power flow equations can be written as

$$\begin{aligned} P_k + P_{Lk} &= 0 \\ Q_k + Q_{Lk} &= 0. \end{aligned} \quad (10)$$

An energy function for the differential algebraic (9) and (10), is given by

$$\mathcal{V}(\tilde{\omega}, \tilde{\delta}, E'_q, V, \tilde{\theta}) = \mathcal{V}_1 + \sum_{k=1}^8 \mathcal{V}_{2k} + C_o \quad (11)$$

where

$$\begin{aligned} \mathcal{V}_1 &= \frac{1}{2} \sum_{k=1}^n M_k \tilde{\omega}_k^2, & \mathcal{V}_{21} &= - \sum_{k=1}^n P_{mk} \tilde{\delta}_k \\ \mathcal{V}_{22} &= \sum_{k=n+1}^{2n+N} P_{Lk} \tilde{\theta}_k, & \mathcal{V}_{23} &= \sum_{k=n+1}^{2n+N} \int \frac{Q_{Lk}}{V_k} dV_k \\ \mathcal{V}_{24} &= \sum_{k=n+1}^{2n} \frac{1}{2x'_{dk-n}} \\ &\quad \cdot [E'_{qk-n} + V_k^2 - 2E'_{qk-n} V_k \cos(\delta_{k-n} - \theta_k)] \\ \mathcal{V}_{25} &= -\frac{1}{2} \sum_{k=n+1}^{2n+N} \sum_{l=n+1}^{2n+N} B_{kl} V_k V_l \cos(\theta_k - \theta_l) \\ \mathcal{V}_{26} &= \sum_{k=n+1}^{2n} \frac{x'_{dk-n} - x_{qk-n}}{4x'_{dk-n} x_{qk-n}} \\ &\quad \cdot [V_k^2 - V_k^2 \cos(2(\delta_{k-n} - \theta_k))] \\ \mathcal{V}_{27} &= - \sum_{k=1}^n \frac{E_f dk E'_{qk}}{x_{dk} - x'_{dk}}, & \mathcal{V}_{28} &= \sum_{k=1}^n \frac{E'_{qk}{}^2}{2(x_{dk} - x'_{dk})}. \end{aligned}$$

$\mathcal{V}_1$  is known as the kinetic energy and  $\sum \mathcal{V}_{2k}$  as the potential energy.  $C_o$  is a constant such that at the post fault stable equilibrium point the energy function is zero.

Using the notation  $[d\mathcal{V}/dt]_{\tilde{\omega}}$  for  $(\partial\mathcal{V}/\partial\tilde{\omega})(d\tilde{\omega}/dt)$ , and similarly for the other states, then we have

$$\begin{aligned} \left[ \frac{d\mathcal{V}_1}{dt} \right]_{\tilde{\omega}} + \left[ \frac{d\mathcal{V}_{21}}{dt} + \frac{d\mathcal{V}_{24}}{dt} + \frac{d\mathcal{V}_{26}}{dt} \right]_{\tilde{\delta}} \\ = - \sum_{k=1}^n D_k (\tilde{\omega}_k)^2 \end{aligned} \quad (12)$$

$$\begin{aligned} \left[ \frac{d\mathcal{V}_{22}}{dt} + \frac{d\mathcal{V}_{24}}{dt} + \frac{d\mathcal{V}_{25}}{dt} + \frac{d\mathcal{V}_{26}}{dt} \right]_{\tilde{\theta}} \\ = \sum (P_k + P_{Lk}) \dot{\tilde{\theta}}_k = 0 \end{aligned} \quad (13)$$

$$\begin{aligned} \left[ \frac{d\mathcal{V}_{23}}{dt} + \frac{d\mathcal{V}_{24}}{dt} + \frac{d\mathcal{V}_{25}}{dt} + \frac{d\mathcal{V}_{26}}{dt} \right]_V \\ = \sum (Q_k + Q_{Lk}) \frac{\dot{V}_k}{V_k} = 0 \end{aligned} \quad (14)$$

$$\begin{aligned} \left[ \frac{d\mathcal{V}_{27}}{dt} + \frac{d\mathcal{V}_{28}}{dt} + \frac{d\mathcal{V}_{24}}{dt} \right]_{E'_q} \\ = - \sum_{k=1}^n \frac{T'_{dok}}{x_{dk} - x'_{dk}} (\dot{E}'_{qk})^2. \end{aligned} \quad (15)$$

Thus, the time derivative of the energy function is

$$\begin{aligned} \frac{d\mathcal{V}}{dt} &= - \sum_{k=1}^n D_k (\tilde{\omega}_k)^2 - \sum_{k=1}^n \frac{T'_{dok}}{x_{dk} - x'_{dk}} (\dot{E}'_{qk})^2 \\ &= \dot{\mathcal{V}}_{NOCSD} \leq 0. \end{aligned} \quad (16)$$

Now assume that a CSD is located between buses  $i$  and  $j$  in the transmission system. The introduction of the CSD does not alter the energy function (11). However, it does alter  $\dot{\mathcal{V}}$ , in particular the terms (13) and (14) no longer sum to zero. To see this, consider the  $i$ th term of (13), i.e.,  $(P_i + P_{Li}) \dot{\tilde{\theta}}_i$ . Without a CSD connected to bus  $i$ ,  $(P_i + P_{Li}) = 0$ , resulting in the zero summation of (13). However when the CSD is connected,

power balance gives  $(P_i + P_{Li} + P_{si}) = 0$ . Therefore, with the CSD connected, the  $i$ th term of (13) becomes  $(P_i + P_{Li})\dot{\theta}_i = -P_{si}\dot{\theta}_i$ . A similar argument follows for the  $j$ th term of (13) and the corresponding terms of (14), resulting in

$$\left[ \frac{dV_{22}}{dt} + \frac{dV_{24}}{dt} + \frac{dV_{25}}{dt} + \frac{dV_{26}}{dt} \right]_{\theta} = -P_{si}\dot{\theta}_i - P_{sj}\dot{\theta}_j \quad (17)$$

$$\left[ \frac{dV_{22}}{dt} + \frac{dV_{24}}{dt} + \frac{dV_{25}}{dt} + \frac{dV_{26}}{dt} \right]_V = -Q_{si} \frac{\dot{V}_i}{V_i} - Q_{sj} \frac{\dot{V}_j}{V_j}. \quad (18)$$

Note that (12) and (15) are unaffected by the introduction of a CSD.

Since all CSD models have  $P_{si} = -P_{sj}$ , the time derivative of the energy function therefore becomes

$$\begin{aligned} \frac{dV}{dt} &= \dot{V}_{NOCS D} + \dot{V}_{CSD} \leq \dot{V}_{CSD} \\ &= -P_{si}\dot{\theta}_{ij} - Q_{si} \frac{\dot{V}_i}{V_i} - Q_{sj} \frac{\dot{V}_j}{V_j}. \end{aligned} \quad (19)$$

This is always valid, irrespective of the generator and load models used in the development of the various energy functions in [8]. Different models contribute different terms to the left hand sides of (17) and (18), but the right hand sides remain unchanged.

Simplification of  $\dot{V}_{CSD}$  for the various devices gives:

**UPFC :**

$$\begin{aligned} \dot{V}_{CSD} &= -b_s V_i \left[ u_1 \frac{d}{dt} (V_i - V_j \cos(\theta_{ij})) \right. \\ &\quad \left. + u_2 \frac{d}{dt} (V_j \sin(\theta_{ij})) \right] \end{aligned}$$

**QBT :**

$$\begin{aligned} \dot{V}_{CSD} &= -b_s \left[ u_q \frac{d}{dt} (V_i V_j \sin(\theta_{ij})) + \frac{1}{2} u_q^2 \frac{d}{dt} (V_i^2) \right] \\ &\approx -b_s u_q \frac{d}{dt} (V_i V_j \sin(\theta_{ij})) \end{aligned}$$

**CSC :**

$$\begin{aligned} \dot{V}_{CSD} &= -\frac{1}{2} b_s u_c \frac{d}{dt} [V_i^2 + V_j^2 - 2V_i V_j \cos(\theta_{ij})] \\ &= -\frac{1}{2} b_s u_c \frac{d}{dt} |\bar{V}_{ij}|^2 = -\frac{1}{2} b_s u_c \frac{d}{dt} [x_L I_{csc} - V_{csc}]^2 \end{aligned}$$

where  $I_{csc}$  is the absolute value of the current through CSC and  $V_{csc}$  is the absolute value of the voltage over CSC.

The energy function will be a CLF, if  $\dot{V}_{CSD}$  is negative. Therefore, the following control (feedback) laws are suggested, (note that  $V_i$  and  $b_s$  are positive):

**Control Law for UPFC :**

$$\begin{aligned} u_1 &= k_1 \frac{d}{dt} (V_i - V_j \cos(\theta_{ij})) \\ u_2 &= k_2 \frac{d}{dt} (V_j \sin(\theta_{ij})) \end{aligned} \quad (20)$$

**Control Law for QBT :**

$$u_q = k_3 \frac{d}{dt} (V_i V_j \sin(\theta_{ij})) \quad (21)$$

**Control Law for CSC :**

$$u_c = k_4 \frac{d}{dt} |\bar{V}_{ij}|^2 = k_4 \frac{d}{dt} [x_L I_{csc} - V_{csc}]^2 \quad (22)$$

where  $k_1$ ,  $k_2$ ,  $k_3$  and  $k_4$  are positive gains which are chosen individually to obtain appropriate damping. Mathematically, any positive gain should stabilize the system. In practice, there are however limitations for these gains, see [1, Section 8.4].

For CSC,  $u_c$  and  $x_c$  have the same sign, see (1). Therefore, in (22)  $u_c$  can be replaced by  $x_c$ , i.e.,

$$x_c = k_5 \frac{d}{dt} |\bar{V}_{ij}|^2 = k_5 \frac{d}{dt} [x_L I_{csc} - V_{csc}]^2. \quad (23)$$

Note that each individual CSD contributes a  $\dot{V}_{CSD}$  term to  $dV/dt$ . If there are a number of CSDs in the system, the overall contribution is the sum of the individual terms. Note also that the control laws (20), (21) and (23) do not require information about the post-fault stable equilibrium point; and rely only on locally measurable information. However, these control laws are in the form of pure derivatives. Therefore, band-pass filters tuned at the frequency range of interest must be used to avoid adverse action of the controller.

Regarding the control law (22), a similar analysis can be found in [9], [10]. For example, using the classical generator model and assuming constant voltages at all buses, the contribution to  $\dot{V}_{CSD}$  of (18) is zero. The control law for a CSC, given by (22), becomes  $u_c = kb_s V_i V_j \sin(\theta_{ij}) \dot{\theta}_{ij} = k_4 \sin(\theta_{ij}) \dot{\theta}_{ij}$ . This control strategy is similar to [10], with the exceptions that it is not a discrete control law and does not require the post fault stable equilibrium point, i.e.,  $P_{ko}$  in [10]. Thus, the control law in [10] is a special case of the general control law (22). The results in [9] are based on the statement ‘‘controllability implies stabilizability.’’ By linearizing the control system, i.e., the system (5), it has been shown in [9] that the linearized system is controllable, and therefore, the control law  $u = u(x)$  is a stabilizer for the linearized system, and also for the nonlinear control system (5). However, the stabilizability of the control laws in this paper is based on the concepts of Control Lyapunov Function and nonlinear system analysis.

#### IV. NUMERICAL EXAMPLE

In this section, two test systems will be used for applying the control laws (20)–(22). Note that these control laws were developed assuming classical Lyapunov modeling, but they will be applied in the examples to ‘‘real’’ systems that are not subject to those modeling restrictions. All simulations are performed by using SIMPOW [11] and the results are plotted in MATLAB.

##### A. Test System I (Two-Area System)

Fig. 3 shows a simple two-area system. The system data can be found in [12, pp. 813–815]. If not otherwise stated, the exact data from [12] is used.

In [12], generators are modeled with one field winding, one damper winding in d-axis and two damper windings in q-axis. Saturation is considered. The active and reactive components of loads have constant current and constant impedance characteristics, respectively. With this example, we would like to study how the various system models affect the performance of the control laws (20)–(22) which are derived from a simplified system, that

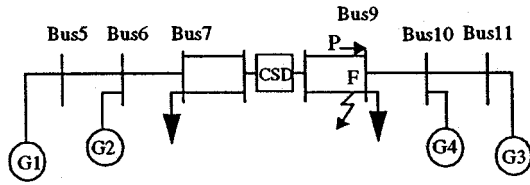


Fig. 3. Simple two-area system.

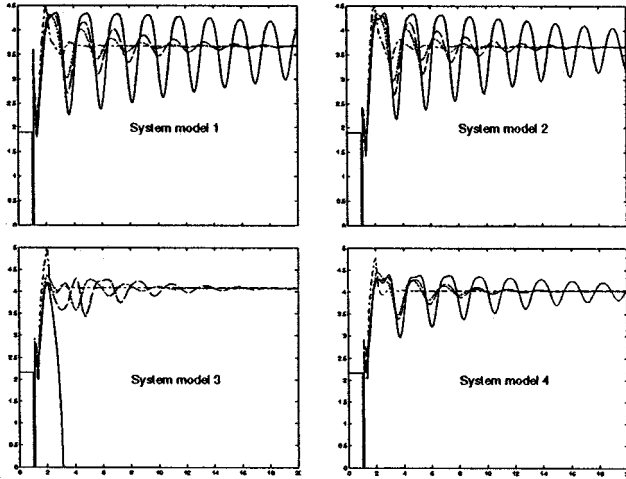


Fig. 4. Variation of  $P$  vs. time in the two-area system.

is, a lossless system in which one-axis model is used for generator and constant real load is considered.

A three-phase fault occurs at point F. The fault is cleared after 100 ms by opening of the faulted line. The following system models will be used in simulation.

*System Model 1:* One-axis model is used for generators ( $D = 2$  p.u.) with excitation system (see [12, Fig. E12.9]).  $K_A = 300$ ,  $T_B = 0.01$  and  $T_R = T_A = 0$ . No PSS.

*System Model 2:* Generators are modeled as in [12] with the same excitation system as in system model 1. Also, turbine and governor regulators are used.  $D = 0$ .

*System Model 3:* The same as in system model 2, but  $P_{G1} = P_{G2} = 730$  MW, i.e.,  $\Delta P_{G1} = \Delta P_{G2} = 30$  MW.

*System Model 4:* The same as in system model 3, but active loads have also constant impedance characteristics.

Fig. 4 shows variation of  $P$  (p.u.) vs. time.  $P$  is the real power through the unfaulted line between the CSD and bus 9, see Fig. 3. The CSDs have the following data. For CSC  $0 \leq x_c \leq 25 \Omega$ , for UPFC  $r_{\max} = 0.094$  p.u and for QBT  $r_{\max} = 0.1$  p.u. The solid curve in Fig. 4 shows  $P$  when there was no CSD. The dotted, dashed and dashdotted curves show  $P$  for CLF control of a UPFC, QBT and CSC, respectively.

The simulation results show the ability of the control laws to stabilize and damp the proposed power system for different system models. System model 3 shows clearly that the CSDs which are controlled by the CLF, enlarge stability region. Obviously, the size of the enlargement depends on the rating of the CSD. For example in system model 3, having the same CSD data, the QBT and UPFC cannot achieve first swing stability when  $P_{G1} = P_{G2} > 740$  MW and for the CSC when  $P_{G1} = P_{G2} > 760$  MW. Also, system model 3 and system

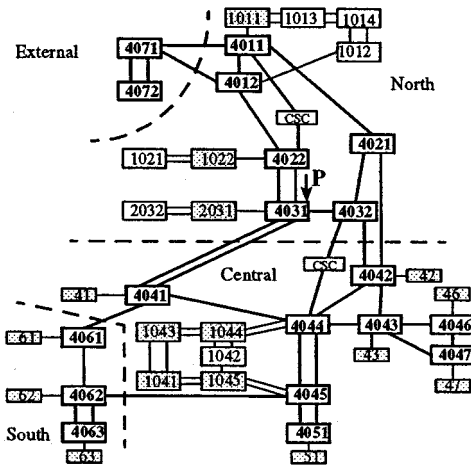


Fig. 5. Nordic32A test system proposed by CIGRE.

model 4 show that the load modeling does not significantly affect the performance of the CLF controlled CSD.

### B. Test System II (Nordic32A)

Nordic32A (Fig. 5) is a test system for simulation of transient stability and long term dynamics proposed by CIGRE Task Force 38.02.08 [13]. The exact data from [13] is used with the exception that no PSS is used in the system. The system contains 32 high voltage buses. The main transmission system is designed for 400 kV. There are also some regional systems at 220 kV and 130 kV. Both hydro power plants and thermal power plants with a total of 23 generators are modeled. The hydro power plants are located in the North and External regions of the system and are equipped with salient pole generators whose models include models of AVR, saturation, one field winding, one damper winding in d-axis and one damper winding in q-axis. The thermal power plants are located in the Central and South regions and each plant includes a round rotor generator whose model includes all features included in the salient pole model but also a second damper winding in q-axis and saturation in the resulting air-gap flux. Only the hydro power units are using governors. The generators have no inherent damping, i.e., the damping constant  $D$  is zero. The active and reactive components of loads have constant current and constant impedance characteristics, respectively.

Two loading cases are considered, namely LF32-028 and LF32-029. In LF32-028, the transfers are high from North to Central. The load level is at peak load. The case is sensitive to many types of faults. In fact the transfer situation is above that recommended by normal reliability standards. LF32-029 is similar to LF32-028 but transfers from North to Central are decreased. It is made by an extra generation at bus 4051 and a decreasing of generating powers in some generators in North.

Two CSCs are used in the system. The first CSC is located in line 4011–4022 and the second one in line 4032–4044. The steady state set points of both CSCs are  $12.8 \Omega$ . For the first CSC,  $8 \leq x_c \leq 30 \Omega$  and for the second one  $8 \leq x_c \leq 20 \Omega$ . Various faults and contingencies have been studied for both LF32-028 and LF32-029. For all cases the CLF controlled CSCs damped power oscillations in an effective and robust manner.

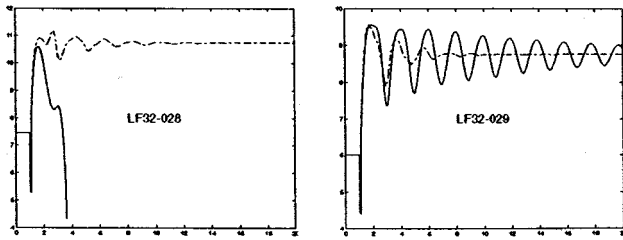


Fig. 6. Variation of  $P$  vs. time in the Nordic32A system.

Also, various load characteristics were applied for this system and simulation results showed that the damping effect of the CLF controlled CSCs was not sensitive to the load modeling. In this paper, we only show the simulation results of one case, that is a three-phase fault imposed on transmission line 4011–4021 at a position very close to bus 4021. The fault is cleared by disconnecting both ends of line 4011–4021 after 100 ms.

In Fig. 6, the solid and dash-dotted curves show variation of  $P$  (p.u), identified in Fig. 5, when the CSCs are uncontrolled, and controlled using CLF, respectively. Note that these two CLF controlled CSCs do not adversely affect each other. The reason is that each device contributes to make the time derivative of the energy function negative.

## V. FUTURE WORK

The model used in the development of the control laws (20)–(22) had a very specific form. It was convenient for obtaining a Lyapunov function, but only approximately describes actual power system behavior. The issue of modeling approximations, and their influence on the stabilization of power systems, is yet to be fully addressed. It is an important focus of the authors' current research. The model (2) will be used to illustrate these ideas.

Assume that the model used in the development of the CLF has the form

$$\dot{x} = f^*(x) \quad (24)$$

whereas the actual system is described by  $\dot{x} = F(x)$ . Simple manipulation gives

$$\dot{x} = F(x) + f^*(x) - f^*(x) = f^*(x) + p(x). \quad (25)$$

Since it is difficult to find a Lyapunov function for (25), a Lyapunov function is derived for (24), i.e., when  $p(x) = 0$ , and a control law established which makes that Lyapunov function a CLF. The following questions arise. How does this control law, derived for (24), affect  $p(x)$ ? In the context of CSD control, how good are the control laws (20)–(22) when the system is lossy, and more detailed models are used for generators and loads?

The simulation results in this paper, and from various other studies, provide a partial answer. They indicate that the control laws are not sensitive to the model approximations. However it is important to obtain an analytical justification of this observation. Theorem 5.3 and the concept of total stability in [2] may provide a partial answer. It remains to extend these theorems to differential algebraic systems.

## VI. CONCLUSION

It has been shown that the Controllable Series Devices (CSD) provide an effective means of adding damping to power systems.

Also, control laws for CSDs based on Control Lyapunov function (CLF) concepts have been derived. The control laws rely only on locally measurable information and are independent of system topology and modeling of power system components. For these control laws, knowledge of post fault stable equilibrium points is not required. Finally, it has also been shown that CSDs with CLF control do not adversely affect each other.

## ACKNOWLEDGMENT

The authors gratefully acknowledge numerous useful comments by M. Noroozian, L. Ångquist and B. Berggren of ABB, M. Danielsson of Svenska Kraftnät and J. Gronquist of PG & E.

## REFERENCES

- [1] M. Ghandhari, "Control Lyapunov functions: A control strategy for damping of power oscillations in large power systems," Ph.D. dissertation, Royal Institute of Technology, TRITA-EES-0004, ISSN 1100-1607, 2000. [Online] Available: <http://media.lib.kth.se:8080/dissengrefhit.asp?dissnr=3039>.
- [2] H. K. Khalil, *Nonlinear Systems*, second ed: Prentice-Hall, Inc., 1996.
- [3] R. A. Freeman and P. V. Kokotovic, *Robust Nonlinear Control Design*: Birkhäuser, 1996.
- [4] A. Bacciotti, *Local Stabilizability of Nonlinear Control Systems*: World Scientific Publishing Co. Pte. Ltd., 1996.
- [5] Z. Artstein, "Stabilization with relaxed controls," *Nonlinear Analysis, Theory, Methods and Applications*, vol. 7, no. 11, pp. 1163–1173, 1983.
- [6] E. Sontag, "A universal construction of Artstein's theorem on nonlinear stabilization," *Systems and Control Letters* 13, pp. 1163–1173, 1983.
- [7] V. Jurdjevic and J. P. Quinn, "Controllability and stability," *Journal of Differential Equations* 28, pp. 381–389, 1978.
- [8] M. A. Pai, *Energy Function Analysis for Power System Stability*: Kluwer Academic Publishers, 1989.
- [9] J. F. Gronquist *et al.*, "Power oscillation damping control strategies for FACTS devices using locally measurable quantities," *IEEE Trans. Power Systems*, vol. 10, no. 3, pp. 1598–1605, 1995.
- [10] K. R. Padiyar and K. Uma Rao, "Discrete control of series compensation for stability improvement in power systems," *Electrical Power & Energy Systems*, vol. 19, no. 5, pp. 311–319, 1997.
- [11] H. R. Fankhauser *et al.*, "SIMPOW—A digital power system simulator," *Reprint of ABB Review*, no. 7, 1990.
- [12] P. Kundur, *Power System Stability and Control*: McGraw-Hill, 1994.
- [13] CIGRE Task Force 38.02.08, "Longer term dynamics phase II," Final report, Jan. 1995.

**Mehrdad Ghandhari** (M'99) received the M.Sc., Tech.Lic. and Ph.D. degrees in electrical engineering from Royal Institute of Technology, Sweden in 1995, 1997, and 2000, respectively. He is currently a Postdoctoral Fellow at the Royal Institute of Technology (KTH), Stockholm, Sweden.

**Göran Andersson** (M'86–SM'91–F'97) received the M.Sc. and Ph.D. degrees from the University of Lund in 1975 and 1980, respectively. In 1980, he joined ASEA's HVDC-division and in 1986 he was appointed professor in Electric Power Systems at the Royal Institute of Technology (KTH), Stockholm, Sweden. Since 2000, he is a Professor at the Federal Institute of Technology (ETH), Zürich, Switzerland.

**Ian A. Hiskens** (S'77–M'80–SM'96) received the B.Eng. and B.App.Sc. (Math) degrees from the Capricornia Institute of Advanced Education, Rockhampton, Australia in 1980 and 1983, respectively. He received the Ph.D. degree from the University of Newcastle, Australia in 1990. He was with the Queensland Electricity Supply Industry from 1980 to 1992 and the University of Newcastle from 1992 to 1999. He is currently a Visiting Associate Professor at the University of Illinois at Urbana-Champaign.